Further, the geometry of the lumen of the α-hemolysin pore will allow the examination of several effects important in organic chemistry, such as the properties of neighboring groups introduced by mutagenesis or targeted chemical modification. Although the present system is restricted to aqueous chemistry on a protein surface, the general principle might be extended to alternative detection methods that work in different environments.

In addition, the electrical signals from reversible covalent-bond-forming reactions are rich in information and could be employed in stochastic sensing[10] to detect organoarsenic species (such as the vesicant lewisite, 2-chlorovinyldichloroarsane) and other reactive molecules, such as nerve and mustard "gases". Because different patterns of residues can be engineered within the lumen of the α-hemolysin pore, the approach should be adaptable to a wide range of chemical systems. Finally, chemical modification at cysteine has played a major role in determining the structures of ion channels in different conformational states.[32–34] It seems likely that reversible chemical modification at cysteine, during single-channel recording, will be valuable in this area too.

Experimental procedures for the preparation of the P_{SH} pore, the synthesis of 4-sulfophenylarsane oxide, and single channel recording are available in the Supporting Information.

Received: July 8, 2002 [Z19685]

[1] X. S. Xie, H. P. Lu, *J. Biol. Chem.* **1999**, *274*, 15967 – 15970.
[2] H. Clausen-Schaumann, M. Seitz, R. Krautbauer, H. E. Gaub, *Curr. Opin. Chem. Biol.* **2000**, *4*, 524 – 530.
[3] A. Engel, D. J. Müller, *Nat. Struct. Biol.* **2000**, *7*, 715 – 718.
[4] A. M. Kelley, X. Michalet, S. Weiss, *Science* **2001**, *292*, 1671 – 1672.
[5] J. M. Fernandez, S. Chu, A. F. Oberhauser, *Science* **2001**, *292*, 653 – 654.
[6] A. Ishijima, T. Yanagida, *Trends Biochem. Sci.* **2001**, *26*, 438 – 444.
[7] H. P. Lu, L. Xun, X. S. Xie, *Science* **1998**, *282*, 1877 – 1882.
[8] X. Zhuang, L. E. Bartley, H. P. Babcock, R. Russell, T. Ha, D. Herschlag, S. Chu, *Science* **2000**, *288*, 2048 – 2051.
[9] R. Yasuda, H. Noji, M. Yoshida, K. Kinosita, H. Itoh, *Nature* **2001**, *410*, 898 – 904.
[10] H. Bayley, P. S. Cremer, *Nature* **2001**, *413*, 226 – 230.
[11] J. A. Mindell, H. Zhan, P. D. Huynh, R. J. Collier, A. Finkelstein, *Proc. Natl. Acad. Sci. USA* **1994**, *91*, 5272 – 5276.
[12] D. C. J. Jaikaran, G. A. Woolley, *J. Phys. Chem.* **1995**, *99*, 13352 – 13355.
[13] M. Goldman, J. C. Dacre, *Rev. Environ. Contam. Toxicol.* **1989**, *110*, 75 – 115.
[14] A. P. Watson, G. D. Griffith, *Environ. Health Perspect.* **1992**, *98*, 259 – 280.
[15] A. H. Smith, C. Hopenhayn-Rich, M. N. Bates, H. M. Goeden, I. Hertz-Picciotto, H. M. Duggan, R. Wood, M. J. Kosnett, M. T. Smith, *Environ. Health Perspect.* **1992**, *97*, 259 – 267.
[16] R. A. Schwartz, *Int. J. Dermatol.* **1997**, *36*, 241 – 250.
[17] W. Lepkowsi, *Chem. Eng. News* **1998**, *76* (46), 27 – 29.
[18] M. M. Rahman, U. K. Chowdhury, S. C. Mukherjee, B. K. Mondal, K. Paul, D. Lodh, B. K. Biswas, C. R. Chanda, G. K. Basu, K. C. Saha, S. Roy, R. Das, S. K. Palit, Q. Quamruzzaman, D. Chakraborti, *J. Toxicol. Clin. Toxicol.* **2001**, *39*, 683 – 700.
[19] M. Reisch, *Chem. Eng. News* **2002**, *80* (6), 9.
[20] Center for Environmental Health Sciences at Dartmouth. www.dartmouth.edu/~toxmwetal/
[21] A. H. Smith, P. A. Lopipero, M. N. Bates, C. M. Steinmaus, *Science* **2002**, *296*, 2145 – 2146.
[22] R. D. Hoffman, M. D. Lane, *J. Biol. Chem.* **1992**, *267*, 14005 – 14011.
[23] R. Moaddel, A. Sharma, T. Huseni, G. S. Jones, R. N. Hanson, R. H. Loring, *Bioconjugate Chem.* **1999**, *10*, 629 – 637.
[24] B. A. Griffin, Ph.D. thesis, University of California, San Diego, **1998**.
[25] B. A. Griffin, S. R. Adams, R. Y. Tsien, *Science* **1998**, *281*, 269 – 272.
[26] S. B. Brown, R. J. Turner, R. S. Roche, K. J. Stevenson, *Biochemistry* **1987**, *26*, 863 – 871.
[27] N. Donoghue, P. T. W. Yam, X.-M. Jiang, P. J. Hogg, *Protein Sci.* **2000**, *9*, 2436 – 2445.
[28] J. Gailer, W. Lindner, *J. Chromatogr. B* **1998**, *716*, 83 – 93.
[29] S. Chouchane, E. T. Snow, *Chem. Res. Toxicol.* **2001**, *14*, 517 – 522.
[30] J. F. Oneto, *J. Am. Chem. Soc.* **1938**, *60*, 2058 – 2059.
[31] E. Moczydlowski in *Ion channel reconstitution* (Ed.: C. Miller), Plenum, New York, **1986**, pp. 75 – 113.
[32] M. H. Akabas, D. A. Stauffer, M. Xu, A. Karlin, *Science* **1992**, *258*, 307 – 310.
[33] M. Holmgren, Y. Liu, Y. Xu, G. Yellen, *Neuropharmacology* **1996**, *35*, 797 – 804.
[34] G. G. Wilson, A. Karlin, *Neuron* **1998**, *20*, 1269 – 1281.

Hydroboration of Coordinated Dinitrogen: A New Reaction for the N_2 Ligand that Results in Its Functionalization and Cleavage**

Michael D. Fryzuk,* Bruce A. MacKay, Samuel A. Johnson, and Brian O. Patrick

An essential process in nitrogen fixation is cleavage of molecular nitrogen.[1] Several studies using model systems have confirmed that metal nitrides can be formed from coordinated dinitrogen providing that at least six electrons are available to formally reduce the N_2 unit to two N^{3-} ligands.[2] To date, all well-characterized molecular examples of metal nitride formation from dinitrogen have involved intermediates containing multiple metal atoms. Therefore, comparisons have been made to the polymetallic FeMoco active site in nitrogenase enzymes, and activated iron surfaces in the Haber process.[3] Herein we report a completely new way to form metal nitrides from coordinated dinitrogen that involves simple organoborane addition to a dinuclear tantalum dinitrogen complex. Because this result is quite unrelated to either biological or industrial nitrogen fixation, we suggest that a new paradigm for both cleaving and functionalizing coordinated dinitrogen is now available.

We have reported the facile preparation of $[\{(NPN)Ta\}_2(\mu\text{-}H)_2(\mu\text{-}\eta^1{:}\eta^2\text{-}N_2)]$ (**1**; where NPN = $(PhNSiMe_2CH_2)_2PPh$),[4] from the spontaneous reaction of N_2 gas with the dinuclear tantalum(IV)–hydride precursor $[\{(NPN)Ta\}_2(\mu\text{-}H)_4]$. Equation (1) shows the 1:1 reaction between dark brown **1** and a THF solution of 9-borabicyclononane (9-BBN), which proceeds to completion over a few hours at room temperature to give orange $[\{(NPN)Ta(H)\}(\mu\text{-}H)_2(\mu\text{-}N_2\text{-}BC_8H_{14})\{Ta(NPN)\}]$ (**2**), in almost quantitative yield.

[*] Prof. Dr. M. D. Fryzuk, B. A. MacKay, S. A. Johnson, Dr. B. O. Patrick
Department of Chemistry
University of British Columbia
2036 Main Mall, Vancouver, BC V6T 1Z1 (Canada)
Fax: (+1) 604-822-2847
E-mail: fryzuk@chem.ubc.ca

[**] We thank the Natural Sciences and Engineering Research Council of Canada for funding.

Supporting information for this article is available on the WWW under http://www.angewandte.org or from the author.

  0044-8249/02/4119-3709 $ 20.00+.50/0

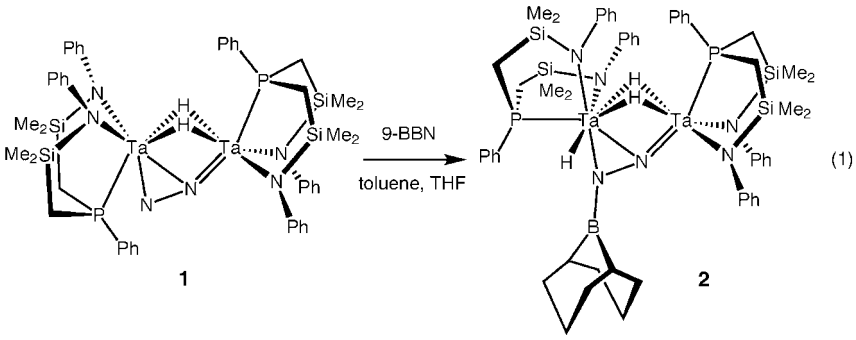

1 2 (1)

The $^{31}P\{^1H\}$ NMR spectra of **1** and **2** each show the presence of a pair of inequivalent phosphane ligands, but the solution ^1H NMR spectrum of **2** indicates C_1 symmetry rather than the C_s symmetry exhibited by **1**. This finding is supported by the solid-state molecular structure of **2**, which was obtained by X-ray diffraction[5] (Figure 1). The N–N bond of the dinitrogen moiety has been elongated from 1.319(4) Å in **1** to 1.411(15) Å in **2**. The B–N bond length is 1.40(2) Å, the sum of the angles around B1 atom is 360.0°, and the sum of angles around N1 is 354.6°. The ditantalum–dinitrogen core of the molecule is nearly planar, with an N1-Ta1-Ta2-N2 torsion angle of −6.3(6)°. The NPN ligand bound to Ta1 appears to be occupying three facial sites with phosphane P1 *trans* to the Ta–Ta axis, amide N3 *trans* to the dinitrogen fragment, and amide N4 *cis* to N3 (angle N3-Ta1-N4 95.3(5)°), which leaves one face of the Ta atom open. Thus, it is likely that the terminal hydride resides on this vacant face.[6] The resonance signal of this hydride is clearly evident at $\delta = 15.31$ ppm in the ^1H NMR spectrum of **2**. Surprisingly, no exchange is observed between the terminal hydride and the two bridging hydride ligands of **2**, either on the NMR timescale as explored by EXSY-NMR spectroscopy or on the chemical timescale in the di-μ-deuterio isotopomer μ-D_2-**2** (prepared from deuterated **1**). We have reported elsewhere[4] that the HOMO of the $[Ta_2(\mu\text{-}\eta^1{:}\eta^2\text{-}N_2)]$ core of **1** has π-bonding character between Ta1 and N1 (numbering as in the structure of **2**), and therefore this reaction can be described as the hydroboration of a metal–dinitrogen π bond. To our knowledge, this B–H addition across a metal–dinitrogen unit is unique, although simple borylations of coordinated dinitrogen have been reported.[7]

The 9-BBN adduct **2** is thermally unstable and gradually undergoes further spontaneous rearrangement. Over four to six weeks in solution, **2** is transformed into the imide–nitride complex **3** (Figure 2) in 42 % yield. Like **2**, the imide–nitride **3** displays C_1 symmetry in solution, as shown by NMR spectroscopic experiments, and in the solid-state as demonstrated by the structure obtained by X-ray crystallography.[5b] The numerous rearrangements leading to **3** include N–N bond scission accompanied by the loss of the three hydride ligands and one phenyl group from an amido donor (see below). Although the ancillary NPN ligand bound to Ta1 has clearly undergone an irreversible rearrangement, the other NPN ligand is unchanged. A highly organized square-planar Ta_2N_2 motif is present in the core of the molecule, with one bridging N atom bound to a Si atom of the rearranged ligand. The borylamido unit of **2** has been transformed into a borylimido fragment with a Ta1–N1 bond of 1.818(5) Å. The solution ^1H NMR spectrum of **3** shows no resonances indicative of hydride ligands, and the observation of D_2 gas (detected by GCMS) in the headspace above solutions of **3** derived from μ-

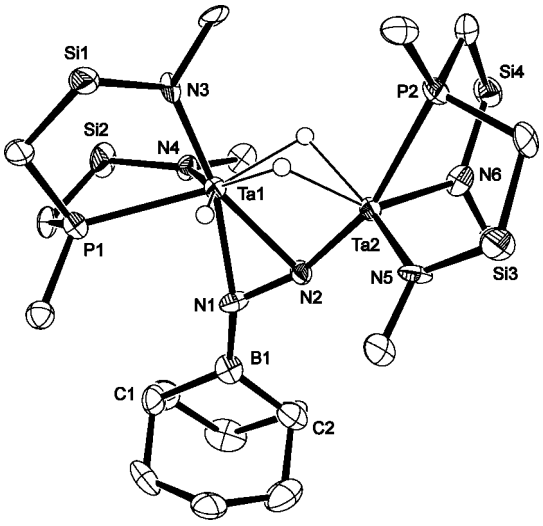

Figure 1. ORTEP drawing of the molecular structure of **2** as determined by X-ray crystallography (thermal ellipsoids set at the 50 % level). Silyl methyl and phenyl ring carbon atoms, other than the ipso carbon atoms, are omitted for clarity. Hydrides were placed using X-HYDEX. Selected bond lengths [Å], bond angles [°], and torsion angles [°]: N1-N2 1.411(15), Ta1-N1 2.123(12), Ta1-N2 2.200(12), Ta2-N2 1.833(11), N1-B1 1.40(2), Ta1-P1 2.583(4), Ta1-N3 2.076(13), Ta1-N4 2.110(11), Ta2-P2 2.606(4), Ta2-N5 2.022(11), Ta2-N6 2.019(12), Ta1···Ta2 2.8483(8); Ta1-N1-N2 73.9(7), 68.0(7), Ta1-N2-Ta 2 89.4(5), Ta1-N1-B1 163.1(10), N1-Ta1-N3 162.0(5), N3-Ta1-N4 95.3(5), N3-Ta1-P1 81.0(3), P1-Ta1-Ta2 152.17(10), N2-Ta2-P2 163.8(4), N5-Ta2-N6 106.0(5); Ta1-N1-N2-Ta2 6.3(6), P1-Ta1-Ta2-P2 −117.8(2), P2-Ta2-Ta1-N2 −174.7(5), P2-Ta2-Ta1-N3 −4.4(4), P2-Ta2-Ta1-N4 106.2(4), B1-N1-N2-Ta1 −168.8(18).

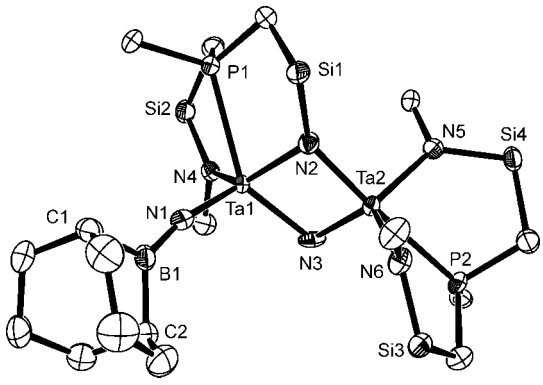

Figure 2. ORTEP drawing of the molecular structure of **3** as determined by X-ray crystallography (thermal ellipsoids set at the 50 % level). Silyl methyl groups and phenyl ring carbons, other than the ipso carbons, are omitted for clarity. Selected bond lengths [Å], bond angles [°], and torsion angles [°]: Ta1-N1 1.818(5), N1-B1 1.404(9), Ta1-N2 2.121(5), N2-Ta2 1.968(5), Ta2-N3 1.826(5), N3-Ta1 1.995(5), N2-Si1 1.717(5), Ta1-N4 2.052(5), Ta1-P1 2.672(2), Ta2-N5 2.062(5), Ta2-N6 2.076(5), Ta2-P2 2.683(1); Ta1-N2-Ta2 99.5(2), N2-Ta2-N3 89.0(22), Ta2-N3-Ta1 99.5(2), N3-Ta1-N2 80.5(2), Ta1-N1-B1 167.0(5), N1-Ta1-P1 102.9(2), N1-Ta1-N4 111.4(2), Ta1-N2-Si1 125.4(3), N3-Ta2-N5 116.3(2), N3-Ta2-N6 116.3(2), N3-Ta2-P2 93.0(2); Ta1-N2-Ta2-N3 −0.5(2), Ta1-Ta2-N2-Si1 174.9(6), N1-Ta1-N2-Ta2 −110.9(2), P1-Ta1-Ta2-P2 143.15(6), Ta2-N2-Ta1-N4 97.1(3).

D_2-**2** indicates the reductive elimination of bridging D groups as D_2 and thus, elimination of bridging hydrides as H_2 from the non-deuterated compounds. The parent dinitrogen complex **1** tolerates several days of reflux in toluene with no elimination or rearrangement of any kind; therefore this intricate transformation is triggered by addition of the organoborane.

The atoms of the dinitrogen unit of **2** apparently correspond to N1 of the boryl imide and bridging nitride N3 of **3**, which implies that the bridging amide N2 is derived from the ancillary NPN ligand by loss of its phenyl substituent. However, the transformations leading to **3** are in fact more complicated. It is relatively simple to prepare $^{15}N_2$-**1** from enriched $^{15}N_2$ and the hydride precursor $[\{(NPN)Ta\}_2(\mu\text{-}H)_4]$, which allows the synthesis of $^{15}N_2$-**2** and $^{15}N_2$-**3**. While ^{15}N NMR spectroscopy is not helpful in exploring the conversion of **2** into **3**, comparison of the ^{29}Si-DEPT NMR spectra of **3** and labeled $^{15}N_2$-**3** unequivocally establishes that a silicon migration occurs during formation of **3**. Unlabeled **3** (top spectrum, Figure 3) gives rise to four doublets in the NMR spectrum (a small two-bond coupling to ^{31}P is observed in all ^{29}Si spectra of the NPN ligand), in agreement with C_1 symmetry which results in four distinct silicon environments. In $^{15}N_2$-**3** (bottom spectrum, Figure 3) one of these signals changes to an AMX doublet of doublets consistent with additional coupling to ^{15}N ($I = 1/2$). Therefore N2 of **3** originates in the dinitrogen ligand of **2**, and the NPN silicon atom Si1 has migrated to it from an NPN-ligand amide. Although there is precedent for intramolecular silicon migration between nitrogen and oxygen atoms of differing nucleophilicity,[8] this is an instance of an amide and a nitride competing for an electrophilic silyl group.

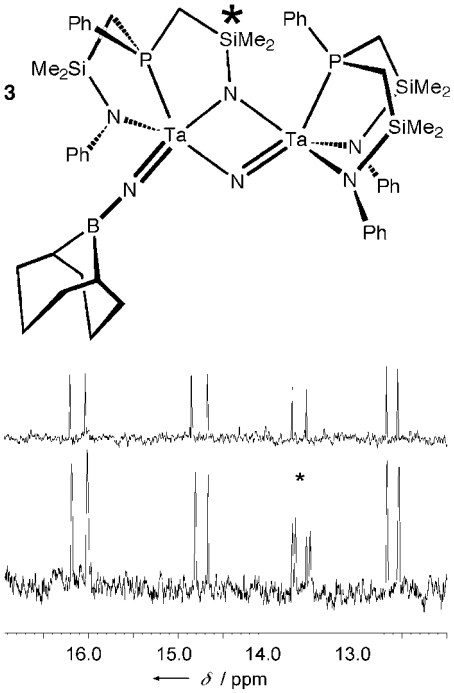

Figure 3. ^{29}Si-DEPT NMR spectra of complex **3** (top) and the isotopomer $^{15}N_2$-**3** (bottom). Additional splitting in the peak at $\delta = 13.64$ ppm (*) is a result of ^{15}N coupling ($I = 1/2$, $^1J_{N,Si} = 3.2$ Hz).

The discovery of an intermediate in the conversion of **2** into **3** supports this assessment and provides further insight into this process. Judicious concentration and cooling of a THF solution of **2** left in a glove box at 15 °C for three weeks produced a crystalline material unlike **2** or **3** by its ^{31}P NMR spectrum. The solid-state molecular structure of **4**[5b] is shown in Figure 4, and, like **3**, it shows the square imide–nitride motif associated with N–N bond cleavage, substantial rearrangement of one NPN ligand, and the absence of hydride ligands bridging the Ta–Ta unit. Although structural parameters for the square Ta_2N_2 motif in **4** are not significantly different from those of **3**, there are two key features of **4** that are not shared with **3**. First, the geometry at B1, which is trigonal planar in **3**,

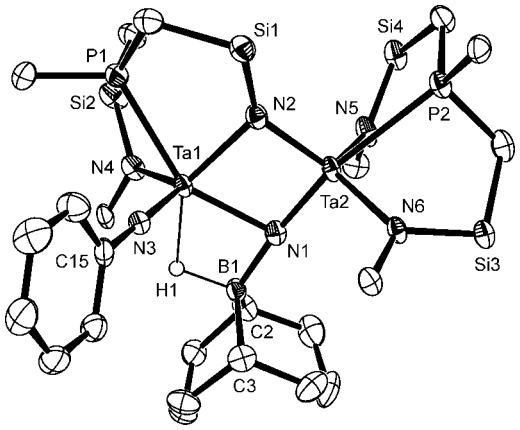

Figure 4. ORTEP drawing of the solid-state molecular structure of **4** as determined by X-ray crystallography (thermal ellipsoids set at the 50% level). Silyl methyl groups and phenyl ring carbon atoms, other than the ipso carbons, are omitted for clarity. Selected bond lengths [Å], bond angles [°], and torsion angles [°]: Ta1···B1 1.92(6), Ta1-N1 2.184(5), Ta1-N2 2.175(5), Ta1-N3 1.793(5), Ta1-N4 2.123(5), Ta1-P1 2.5900(15), N1-B1 1.517(8), B1-H1 1.33(6), Ta1-H1 1.92(6), N2-Si1 1.737(5), N1···N2 2.737(4), Ta2-N5 2.049(5), Ta2-N6 2.111(5), Ta2-P2 2.7831(15); N1-Ta1-N2 77.76(17), Ta1-N2-Ta2 93.66(18), N2-Ta2-N1 92.3(2), Ta2-N1-Ta1 96.20(19), Ta1-N1-B1 88.0(3), N1-B1-H1 101(3), N1-Ta1-N3 113.74(19), N1-Ta1-N4 109.26(18), N1-Ta1-P1 148.57(12), N1-Ta2-N5 101.93(19), N1-Ta2-N6 99.84(19), N1-Ta2-P2 167.80(15); Ta1-N2-Ta2-N1 −2.7(2), P1-Ta1-Ta2-P2 346.9(1), N1-Ta1-N2-Si1 163.2(3), N2-Ta1-N1-B1 −170.8(3).

is roughly tetrahedral in **4** as a result of the presence of the bridging hydride H1, which was located in the diffraction experiment and gives a resonance signal at $\delta = 4.56$ ppm in the ^{1}H NMR spectrum of **4**. H1 is presumably involved in an agostic interaction with Ta1 (Ta1···B1 = 1.92(6) Å, N1-B1-H1 = 101(3)°). The second and most significant difference between **3** and **4** is the linear phenylimido moiety of **4**, which is the fragment expected to result from the silyl group migration off the NPN-ligand amide group and onto a dinitrogen-derived nitride ligand. After the migration, the boron hydride and the phenyl group bound to former NPN ligand amide N3 are then arranged in a manner that allows for elimination of benzene, a requirement for formation of **3** from **4**. The elimination of the boron hydride with the phenyl substituent of N3 as benzene can be detected by ^{1}H and ^{13}C NMR spectroscopy—both benzene and **3** can be identified in [D_8]THF solutions of **4** after a few days. This benzene elimination would leave N3 as a terminal nitride ligand. One

  0044-8249/02/4119-3711 $ 20.00+.50/0

final question arises: does this nitride (N3) attack the other Ta atom (Ta2), displacing the bridging N1-BC_8H_{14} moiety to a new position as the terminal and linear imidoborane seen in **3**, or does it simply acquire the BC_8H_{14} group from the bridging nitride N1 in **4** to give **3**? The labeling study described above indicates that the former occurs, and that the B1–N1 bond remains intact throughout these transformations. Compared to the ^{11}B NMR spectrum of **3**, the ^{11}B spectrum of $^{15}N_2$-**3** shows a poorly resolved splitting attributed to ^{15}N–^{11}B coupling. The considerable strength of the B–N bond[9] makes this rearrangement more likely than migration of the borabicyclononyl fragment. Therefore N1 and N2 in **3** are dinitrogen-derived atoms.

A proposed mechanism for the transformation of **2** into **3** is shown in Scheme 1. Considering the overall reaction as the initial formation of **1** from $N_{2(g)}$ and tantalum(IV) hydride precursor $[\{(NPN)Ta\}_2(\mu\text{-}H)_4]$, this system achieves the six-electron reduction of the N_2 unit in a stepwise fashion, with a number of isolatable intermediates and detectable byproducts. As discussed previously, the first four electrons required for activation of N_2 to N_2^{4-} derive from elimination of two bridging hydride ligands as H_2 and from a Ta^{IV}–Ta^{IV} bond (which is itself derived by H_2 elimination from the Ta^V starting material $[(NPN)TaMe_3]$ following hydrogenation).[4] This is the reaction between the precursor and N_2 to generate **1**. We suggest that reductive elimination of H_2 from **2** provides the last two electrons for the overall six-electron reduction of the N_2 unit to two N^{3-} nitride units. Remarkably, the six electrons required to cleave the N_2 unit were all obtained by reduction of hydride ligands to H_2 gas.

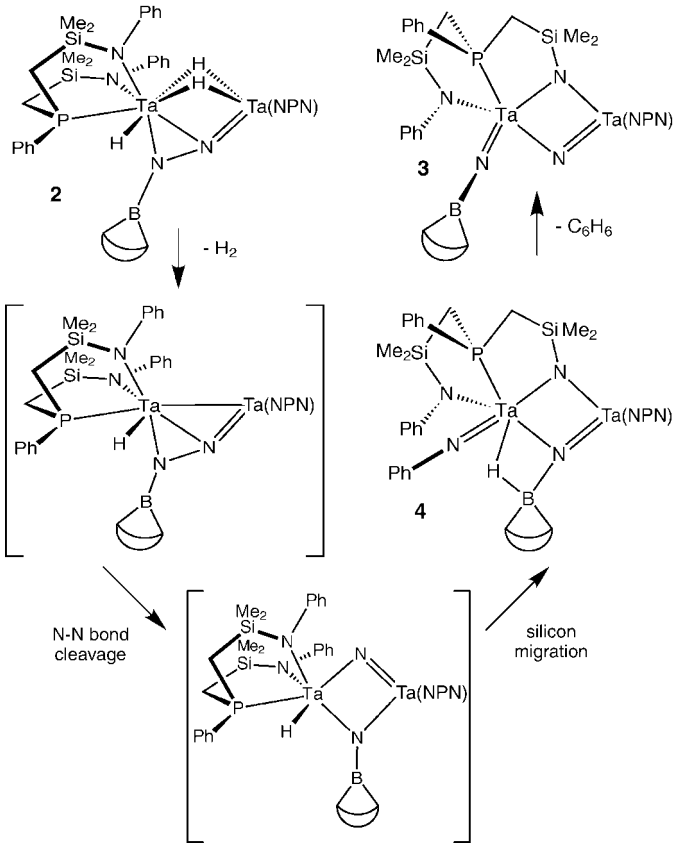

Scheme 1.

In conclusion, a new reaction for coordinated dinitrogen has been explored, in which a B–H bond adds across a Ta–N bond to give a complex with a functionalized N_2 ligand and a new terminal hydride ligand. The spontaneous transformations of this complex result from H_2 elimination and N–N bond cleavage, which lead to dinitrogen-derived nitride ligands. While such processes are unique reactivity patterns in dinitrogen chemistry, the irreversible ligand degradation that occurs limits the usefulness of this reaction. Nevertheless, experiments to extend this chemistry using modified ancillary NPN ligands and different primary and secondary alkylboranes are underway.

Complete experimental details are available in the Supporting Information.

Received: July 9, 2002 [Z19695]

[1] a) T. Travis, *Chem. Ind.* **1993**, *51*, 581–585; b) M. D. Fryzuk, S. A. Johnson, *Coord. Chem. Rev.* **2000**, *200–202*, 379–409; c) S. Gambarotta, *J. Organomet. Chem.* **1995**, *500*, 117; d) M. Hidai, Y. Mizobe, *Chem. Rev.* **1995**, *95*, 1115; e) C. E. Laplaza, C. C. Cummins, *Science* **1995**, *268*, 861.

[2] a) C. C. Cummins, *Chem. Commun.* **1998**, *17*, 1777–1786; b) E. E. van Tamelenn, *Acc. Chem. Res.* **1970**, *3*, 361; c) M. E. Vol'Pin, M. A. Ilatovskaya, L. V. Kosyakova, V. B. Shur, *J. Chem. Soc. Chem. Commun.* **1968**, 1074; d) E. Solari, C. Da Silva, B. Iacono, J. Hesschenbrouck, C. Rizzoli, R. Scopelliti, C. Floriani, *Angew. Chem.* **2001**, *113*, 4025–4027; *Angew. Chem. Int. Ed.* **2001**, *40*, 3907–3909; e) V. M. E. Bates, G. K. B. Clentsmith, F. G. N. Cloke, J. C. Green, D. L. Huw, *Chem. Commun.* **2000**, *11*, 927–928; f) A. Caselli, E. Solari, R. Scopelliti, C. Floriani, N. Re, C. Rizzoli, A. Chiesi-Villa, *J. Am. Chem. Soc.* **2000**, *122*, 3652–3670; g) G. K. B. Clentsmith, V. M. E. Bates, P. B. Hitchcock, F. G. N. Cloke, *J. Am. Chem. Soc.* **1999**, *121*, 10444–10445.

[3] a) J. M. Smith, R. J. Lachicotte, K. A. Pittard, T.R Cundari, G. Lukat-Rodgers, K. R. Rodgers, P. L. Holland, *J. Am. Chem. Soc.* **2001**, *123*, 9222–9223; b) D. Sellmann, B. Hautsch, A. Rosler, F. W. Heinemann, *Angew. Chem.* **2001**, *113*, 1553–1555; *Angew. Chem. Int. Ed.* **2001**, *40*, 1505–1507; c) Q. F. Zhang, L. C. Joyce, W. Lai, W.-T. Lai, W.-H. Leung, *Inorg. Chem.* **2001**, *40*, 2470–2471; d) Y. Nishibayashi, I. Wakiji, K. Hirata, M. R. DuBois, M. Hidai, *Inorg. Chem.* **2001**, *40*, 578–580; e) T. L. Haslett, S. Fedrigo, K. Bosnick, M. Moskovits, H. A. Duarte, D. Salahub, *J. Am. Chem. Soc.* **2000**, *122*, 6039–6044; f) T. Dube, S. Conochi, S. Gambarotta, G. P. A. Yap, G. Vasapollo, *Angew. Chem.* **1999**, *111*, 3890–3892; *Angew. Chem. Int. Ed.* **1999**, *38*, 3657–3659; g) D. Sellmann, A. Fursattel, *Angew. Chem.* **1999**, *111*, 2142–2145; *Angew. Chem. Int. Ed.* **1999**, *38*, 2023–2026; h) T. H. Rod, B. Hammer, J. K. Norskov, *Phys. Rev Lett.* **1999**, *82*, 4054–4057.

[4] M. D. Fryzuk, S. A. Johnson, B. O. Patrick, A. Albinati, S. A. Mason, T. F. Koetzle, *J. Am. Chem. Soc.* **2001**, *123*, 3960–3973.

[5] a) The solid-state molecular structure obtained for **2** features two discrete molecules, one of each possible enantiomeric form. These two molecules are isostructural and we report parameters for one of them throughout this paper. b) Information regarding collection, solution, and refinement of this data is summarized in the Supporting Information. CCDC-188057 (**2**), CCDC-188056 (**3**), CCDC-188058 (**4**) contains the supplementary crystallographic data for this paper. These data can be obtained free of charge via www.ccdc.cam.ac.uk/conts/retrieving.html (or from the Cambridge Crystallographic Data Centre, 12, Union Road, Cambridge CB21EZ, UK; fax: (+44) 1223-336-033; or deposit@ccdc.cam.ac.uk).

[6] The terminal hydride was successfully modeled using XHYDEX at a Ta–H separation of 1.6 Å. For XHYDEX, see A. G. Orpen, *J. Chem. Soc. Dalton Trans.* **1980**, 2509.

[7] H. Ishino, Y. Ishii, M. Hidai, *Chem. Lett.* **1998**, 677–678.

[8] a) M. Abe, Y. Shirodai, Y. , M. Nojima, *J. Chem. Soc. Perkin Trans. 1* **1998**, *19*, 3253–3260; b) M. D. Fryzuk, P. A. MacNeill, *J. Am. Chem. Soc.* **1984**, *106*, 6993–6999.

[9] *Encyclopedia of Inorganic Chemistry* (Ed.: R. B. King), Wiley, Chichester, **1994**, p. 302.

  0044-8249/02/4119-3712 $ 20.00+.50/0